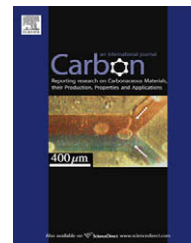


available at [www.sciencedirect.com](http://www.sciencedirect.com)journal homepage: [www.elsevier.com/locate/carbon](http://www.elsevier.com/locate/carbon)

# Substrate-free synthesis of large area, continuous multi-layer graphene film

Fang Liu, Yong Zhang \*

School of Materials Science and Engineering, Dalian Jiaotong University, 794 Huanghe Road, 116028 Dalian, PR China

## ARTICLE INFO

### Article history:

Received 27 May 2009

Accepted 22 February 2010

Available online 25 February 2010

## ABSTRACT

Large area ( $\sim\text{cm}^2$ ) multi-layer graphene film is synthesized in the substrate-free vapor phase. The scanning electron microscopy observation reveals that the graphene nanoflakes are either six- or five-sided, and the internal angles between adjacent sides are nearly  $120^\circ$  and  $105^\circ$ , respectively. The nucleation of hexagonal and pentagonal carbon rings leads to carbonaceous nuclei, which grow into six- or five-sided nanoflakes, respectively. A well-ordered and large-area graphene monolayer is formed by the interconnection of these flakes, and stacking of these monolayers results in the formation of a multi-layer graphene film. The creation of hexagonal and pentagonal carbon rings is considered to be important for the easy production of large area multi-layer graphene at large scale.

© 2010 Elsevier Ltd. All rights reserved.

## 1. Introduction

In recent years, graphene has become the newly attractive subject in nanomaterials science, because of its unique nanostructure and unusual electronic, mechanical, thermal conductive properties, etc. [1–3]. For the purpose of fundamental study and technological application, synthesis of low cost and large-area graphene is highly desirable. Since the firstly successful fabrication of graphene by cleavage [4], generally three major methods for the fabrication of single and multi-layer graphene have been investigated, and these methods include the micromechanical cleavage or chemical exfoliation of graphite [4], thermal decomposition of SiC [5] and chemical vapor deposition (CVD) of hydrocarbons on substrate surface [6].

Among the three existing methods, mechanical or chemical exfoliation of bulk graphite always resulted in limited area of graphene. In the case of thermal decomposition of SiC, the graphene exhibited poor uniformity and contained a multitude of domains. In the CVD case, some investigations on the CVD synthesis of graphene have been reported [6–8], with

the successful formation of graphene on some substrates. However, strong bonding between graphene and corresponding substrate not only significantly alters the transport properties of graphene [9], but also complicates the separation of graphene from substrate surface. The simple synthesis of low cost and large-area graphene is still a big challenge.

As is well known, various carbon nanostructures, such as carbon nanotubes (CNTs) and diamond have been successfully synthesized in the vapor phase at large scale, without the assistance of substrate [10–12]. Since graphene is the mother of various carbon materials, graphene may also be synthesized in the substrate-free vapor phase, by selecting reasonable carbon precursor and reaction conditions. Not only the influence of substrate on the transport properties of graphene will be eliminated, but also the synthesis process of graphene will be greatly simplified. However, only Dato et al. [6] have reported the substrate-free gas phase synthesis of graphene, and the large-area graphene has not been achieved. In this paper, large area ( $\sim\text{cm}^2$ ) multi-layer graphene film was synthesized in the substrate-free vapor phase, and its forming mechanism was discussed.

\* Corresponding author. Fax: +86 0411 84106828.

E-mail address: [zhangyong0411@126.com](mailto:zhangyong0411@126.com) (Y. Zhang).

0008-6223/\$ - see front matter © 2010 Elsevier Ltd. All rights reserved.

doi:10.1016/j.carbon.2010.02.033

## 2. Experimental

The experimental scheme of substrate-free synthesis of graphene is shown in Fig. 1. A one-meter long quartz tube, horizontally placed inside a horizontal furnace, was used as the CVD reactor, and the two sides of long quartz tube was sealed by rubber plugs. Firstly, the camphor was placed inside the quartz tube, with argon as carrier gas at ambient pressure. When heated above 180 °C, the camphor was evaporated. Then, the evaporated camphor was pyrolyzed during 800–850 °C in the furnace. After 40 min reaction, the film products were adhered to chamber wall, which were easily peeled off in large area. Many separated large area films were also found from middle position of the quartz tube to its argon outlet place. In order to understand the nucleation mechanism, the reaction products were annealed at 600 °C under N<sub>2</sub> flow for 20 min, and it took 20 min to increase the temperature from room temperature to 600 °C.

The reaction products collected in the quartz tube were studied using scanning electron microscopy (SEM, JSM-6360LV), X-ray diffraction (XRD, D/Max-Ultima<sup>+</sup>) and high-resolution transmission electron microscopy (HRTEM, JEOL2010). Scanning tunneling microscopy (STM, CSPM4000) was recorded in air at ambient temperature. Raman spectroscopy was performed at room temperature with a Renishaw spectrometer using a 514.5 nm laser, with a spot size of 1 μm and a low excitation power of 0.2 mW to minimize sample heating.

## 3. Results and discussion

An optical image of the as-prepared film, taken by the digital camera, is shown in Fig. 2a. Obviously, large area of about 1 cm × 1 cm film is obtained, which looks very smooth and continuous. In addition, different optical transparency in different regions can be seen, which may be resulted from the crumpling or overlapping of graphene layers.

Typical low-magnification and high-magnification SEM observations of the as-prepared film are demonstrated in Fig. 2b and c, respectively. As can be seen, regular shaped nanoflakes exhibiting well-faced sides are clearly identified, and the diameter is about 2–3 μm (Fig. 2b). Moreover, the internal angle between adjacent well-faced sides is nearly 120° or 105° (Fig. 2c), which is close to the internal angle of hexagon or pentagon, revealing that the nanoflakes are mostly six-sided or five-sided, respectively. A slight deviation from the angle of 120° or 105° may be resulted from the jostle

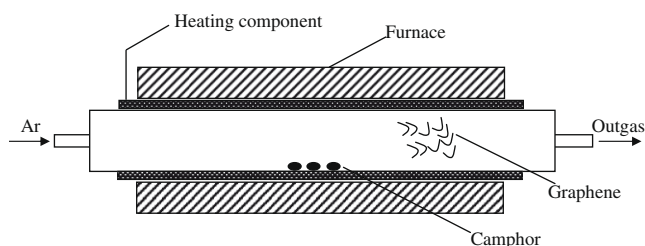


**Fig. 1 – Experimental scheme of substrate-free synthesis of graphene film.**

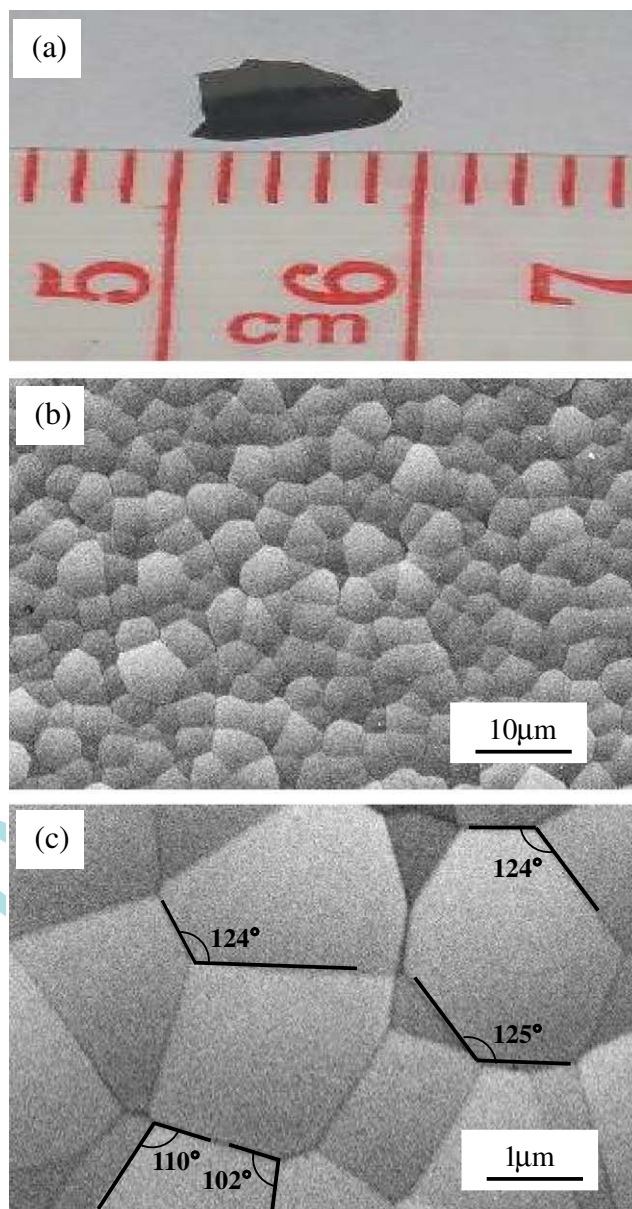


**Fig. 2 – Micrographs of the as-prepared film. (a) Optical image; (b) and (c) SEM images.**

and distortion among densely interconnected nanoflakes. In addition to the six-sided and five-sided nanoflakes, several other shape polygonal nanoflakes are also seen in Fig. 2c.

Fig. 3 presents the HRTEM observation for the as-prepared film obtained by substrate-free vapor phase. As shown in Fig. 3a and b, the low-magnification and medium-magnification images both reveal the flake-like morphology of folded graphene in some regions, showing relative dark features. Previous TEM observations [13,14] of graphene have proven that the transparent and featureless regions were monolayer graphene, and less transparent areas were attributed to the folding of single sheet or overlapping of multiple graphene layers, to fulfill their thermodynamic stability. Therefore, different optical transparency in different regions of the graphene film is observed, as shown in Fig. 2a. In addition, polyhedral shape graphene is also seen in Fig. 3c, in agreement

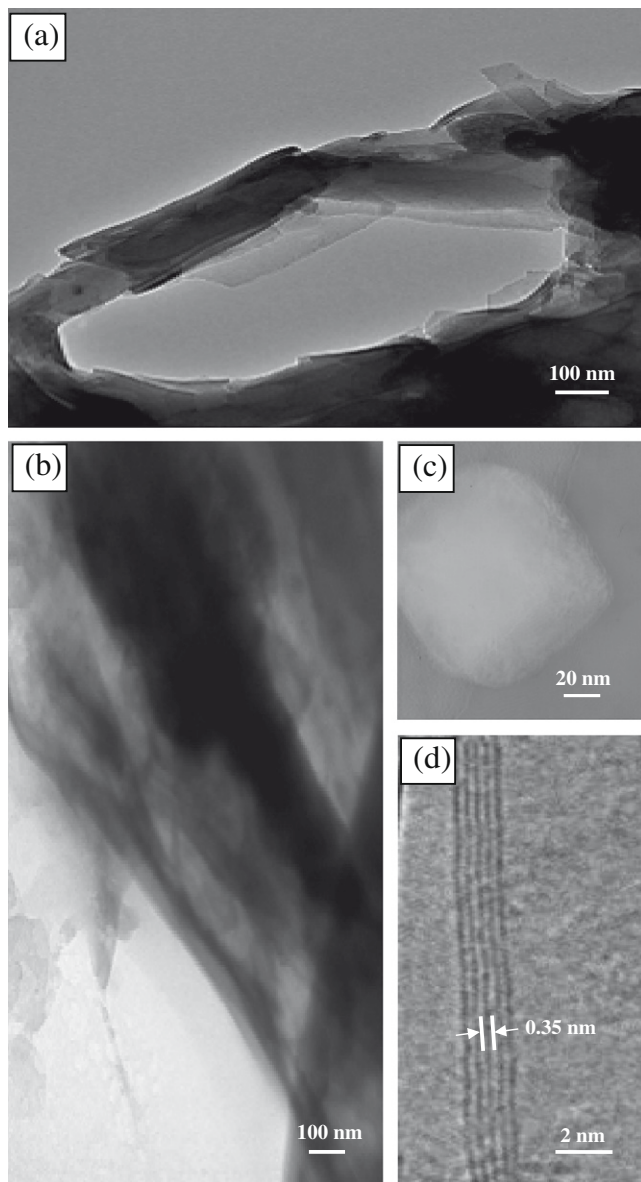


**Fig. 3 – HRTEM images of the as-prepared film. (a) Low-magnification image; (b) medium-magnification image; (c) high-magnification image showing the layer stacking.**

with the SEM observation of Fig. 2. Furthermore, the stacking layers of graphene in the high-magnification image of Fig. 3d are clearly seen. The plane spacing measured from different nanoflakes is about 0.35 nm, which is consistent with the theoretical value of 0.34 nm in graphite, confirming the formation of multi-layer graphene in this paper.

To obtain further information about the surface structure of graphene film, STM observation is performed, as shown in Fig. 4. Clearly, the topographic image of Fig. 4a illustrates that an atomic-scale smooth film surface is obtained. The high-resolution STM image of its inset further demonstrates the appearance of hexagonal lattice, also confirming the formation of graphene layer in this paper. Moreover, a threefold symmetry (“three-for-six”) pattern [15] in the high-resolution STM image is observed, that is, three bright or dark features can be seen for each set of six carbon atoms, consistent with

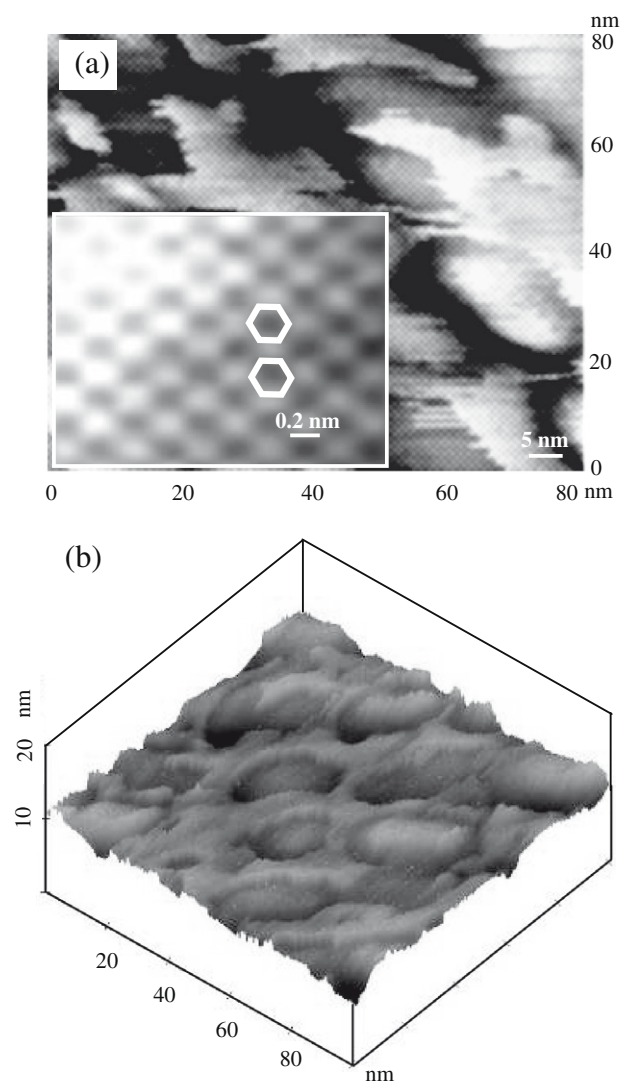


**Fig. 4 – STM observation of graphene film (a) topographic images of different regions of graphene, with inset being a high-resolution image; (b) stereographic image.**

previous result of graphene [15]. Fig. 4b is the stereographic STM image of graphene film. It is constructed by the polyhedra of different shape and a relatively modest height fluctuation can be clearly observed, in agreement with the polyhedron and slight folding of graphene in the HRTEM observation.

Raman spectroscopy is performed from two different places of the sample at room temperature, as shown by the real line and dashed line spectra in Fig. 5a. Three peaks centered at 1336, 1587 and 2778  $\text{cm}^{-1}$  of real line spectrum, can be obviously seen, which are assigned to the D, G and 2D modes of graphene, respectively. Similarly, three peaks centered at 1334, 1594 and 2780  $\text{cm}^{-1}$  of dashed line spectrum are also shown. Usually, the D/G ratio has always been used to characterize the structure integrity of carbon materials, and the increase of D/G ratio is resulted from the increase of defects or structural disorder. As far as graphene is concerned, the defects include vacancies and distortions which may be attributed to non-uniformity, corrugation and twisting in

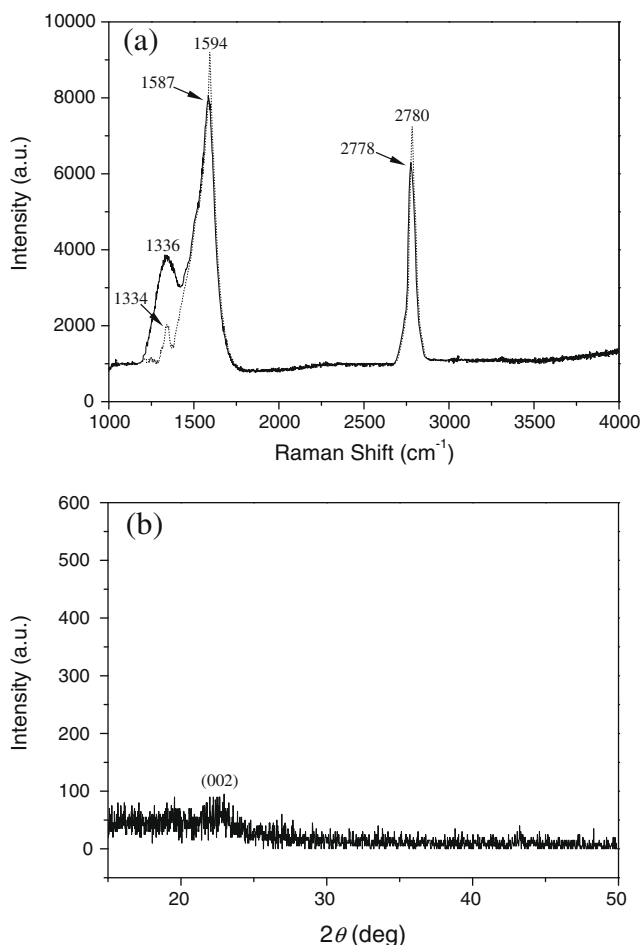


**Fig. 5 – (a) Raman spectroscopy and (b) XRD pattern of graphene film grown by substrate-free CVD.**

graphene sheets [16]. As shown in Fig. 5a, small D/G ratio is obtained, indicating the good crystallinity of graphene obtained in this paper. XRD pattern of the obtained sample (Fig. 5b) exhibits a weak and broad peak at about 23°, which is corresponded to the (0 0 2) crystal plane of graphene, also indicating its good crystallinity [17].

Moreover, the shape and position of 2D peak can be used to clearly distinguish single-layer, bilayer and few-layer graphene [18]. Single-layer graphene usually has a single and sharp 2D peak below 2700 cm<sup>-1</sup>, and bilayer graphene exhibits a broader and upshifted 2D peak located at 2700 cm<sup>-1</sup>. In the case of graphene sheets with more than five layers, they exhibit broad 2D peaks that are upshifted to positions greater than 2700 cm<sup>-1</sup>, similar with bulk graphite. For this reason, the graphene film obtained in this paper is the multi-layer case.

Based on the above results, large area multi-layer graphene is synthesized in this paper, and its large area advantages are related to its formation mechanism. Generally, the formation of graphene on substrate surface during CVD is mainly composed of nucleation and growth stages [7,19]. Firstly, carbon dimers or trimers produced during pyrolysis are absorbed on the substrate surface and form different carbon structures. Then, heteroepitaxial growth of ordered graphite structure is driven by the lattice matching between substrate surface and

graphene, resulting in some heteroepitaxial island on the substrate. Subsequently, separate islands meet and join each other to form a smooth graphene film. Because of the difference of thermal expansion coefficients between graphene and substrate surface, mechanical stress will appear during the cooling process, leading to the formation of ridges or swells as reported previously [20,21].

In this case, the lattice matching between substrate surface and graphene is a critical factor for the growth of graphene. Up to now, only a portion of substrates [10,11] have been found to grow graphene. Furthermore, the strong bonding between graphene and substrate substantially alters the electronic structure of graphene, as well as complicating the separation process of graphene sheets.

It is well known that, the nucleation and growth of graphene in the vapor phase is a typical vapor–liquid–solid (VLS) process, which is in accordance with the smallest energy principle during reaction. That is, the formation of graphene should be along its easiest growth direction. Since graphene exhibits hexagonal lattice structure, the [0 0 0 1] direction is the closest packed plane [22,23], and stacking of hexagonal or pentagonal carbon rings along the [0 0 0 1] direction thus becomes the most energetically favorable. As shown in Fig. 6, abundant hexagonal and pentagonal carbon rings can be formed from the breaking of camphor molecule during pyrolysis [11]. Then, the nucleation of hexagonal carbon rings leads to the formation of carbonaceous nuclei. With the continuous coming of hexagonal carbon rings, the carbonaceous nuclei grow into six-sided nanoflakes. Also, the nucleation and growth of pentagonal carbon rings result in five-sided nanoflakes in the similar way. Subsequently, the joining of

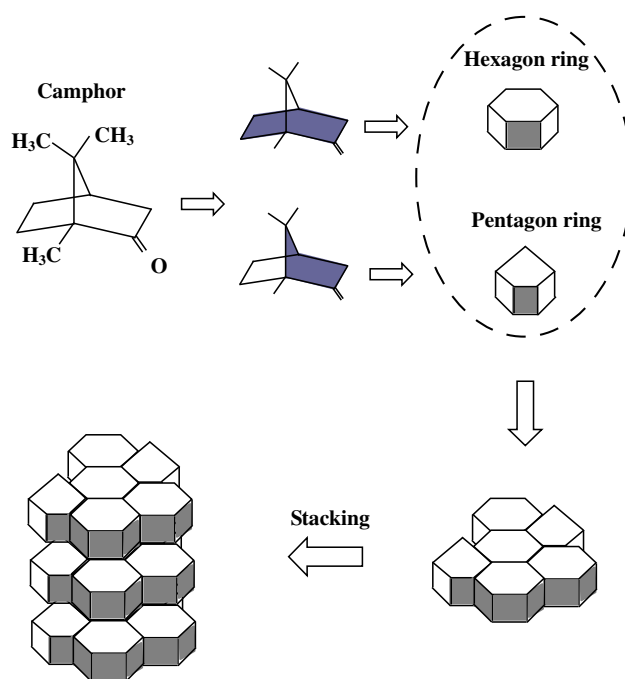


**Fig. 6 – Scheme of the growth model for the multi-layer graphene film. The formation of hexagonal or pentagonal ring, as well as the formation of graphene multilayer film is demonstrated.**

six-sided and five-sided nanoflakes forms the well-ordered and large-area graphene monolayer, as shown in Fig. 6.

Different from the formation process of graphene on substrate surface, stress release between graphene and substrate does not exist, and no ridges or swells are found. Regular shaped six-sided and five-sided graphene nanoflakes are formed, as demonstrated in Fig. 2b and c. Furthermore, stacking of these monolayers along the [0 0 0 1] direction results in the formation of multi-layer graphene film.

The identification of nucleation sites is of great importance to understand the nucleation mechanism. Lee et al. [24], have identified the nucleation sites of diamond growth, by etching of nondiamond carbon binder and leaving only nanodiamond nuclei. Because amorphous carbon species and impurities always exist at the grain boundary of carbon films [25], and the chemical reactions of them during annealing will degradate the internal grain boundaries [25,26], leaving only crystalline carbon species, annealing of carbon film is also a simple and effective method to know the nucleation sites of carbon films.

In reference of previous report [26], the multi-layer graphene film prepared in this paper was annealed at 600 °C under N<sub>2</sub> flow, and its SEM observation is shown in Fig. 7. Obviously, degradation of the internal grain boundaries can be seen in Fig. 7a and b, leaving six-sided, five-sided and other shape

polyhedra (Fig. 7c and d), which indicates the nucleation of hexagonal and pentagonal carbon rings into carbonaceous nuclei. The existence of polyhedra from small to big in Fig. 7c and d may reveal that, carbonaceous nuclei of nanometer scale can firstly become small and thin nanoflakes, then grow into big and thick flakes of micrometer scale. Moreover, Fig. 7c demonstrates that, the five-sided and other shape polyhedra are joined each other, indicating the joining behavior of polyhedral shape nanoflakes to form monolayer graphene. Fig. 7e and f further exhibit the stacking phenomenon of joined polyhedra, indicating the stacking behavior of monolayer graphene to form multi-layer graphene. The construction of polyhedral nanoflakes results in the two dimensional polygonal microstructure (Fig. 2c) and three dimensional height fluctuating surface (Fig. 4b), confirming the above nucleation mechanism proposed in this paper.

Obviously, the formation of large area multi-layer graphene by substrate-free vapor phase, is largely depends on the creation of hexagonal or pentagonal carbon rings. Though Dato et al. [6] has reported the substrate-free gas phase synthesis of graphene sheets, ethanol was used as carbon source in that case. Since no hexagonal or pentagonal carbon rings are created from the breaking of ethanol molecule, large area multi-layer graphene film is not obtained. Somani et al. [8] has synthesized graphene by CVD of camphor on Ni

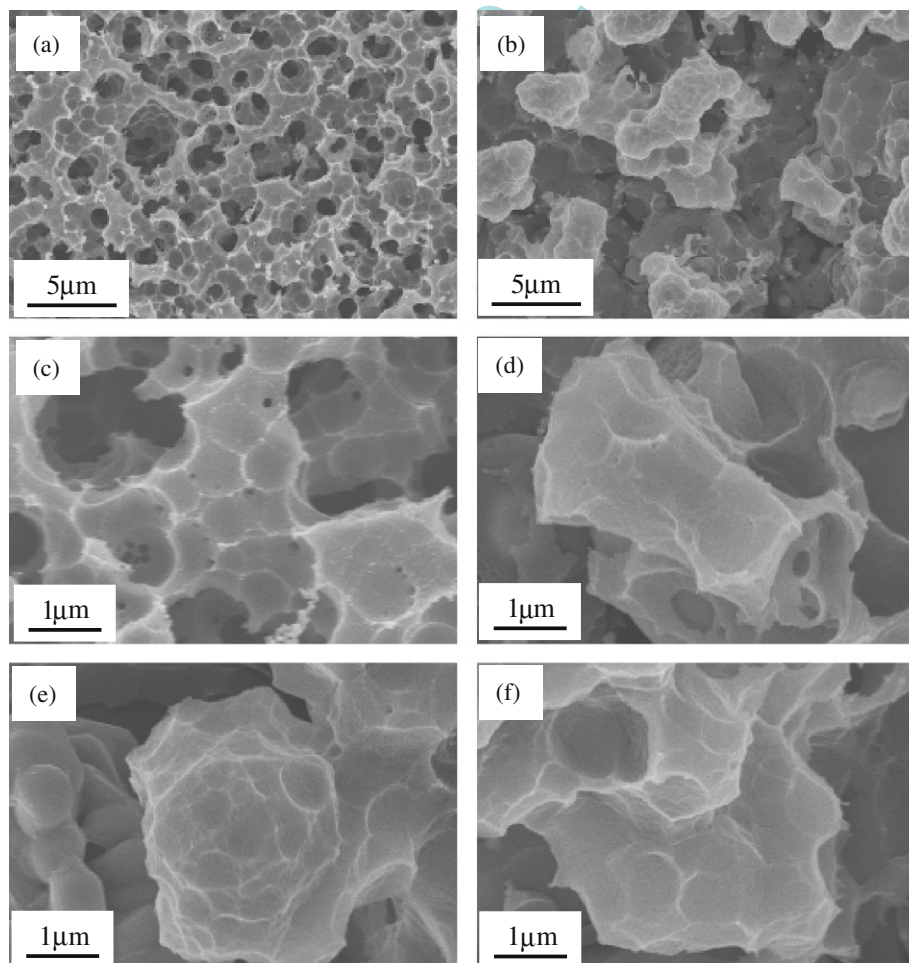


Fig. 7 – SEM observation of the multi-layer graphene film after 600 °C annealing under N<sub>2</sub> flow.

substrate. However, no six-sided or five-sided graphene nanoflakes were found, perhaps due to the lattice matching between graphene and Ni substrate.

It has been reported that [27], small monocyclic carbon rings coalesced to form polycyclic rings, and subsequently converted to fullerenes. Kiang and Goddard [28] demonstrated that the growth of single-layer CNTs were also started from the small monocyclic carbon rings, during the vapor phase grown process. Another growth mechanism of CNTs [29] suggested the incorporation of carbon dimmers into a cage-like precursor. Moreover, Frenklach et al. reported that, hexagonal-like nanoparticles were obtained by the homogeneous nucleation of diamond in vapor phase [12]. Because graphene is the basic structure of fullerenes, CNTs and other carbonaceous materials, these experimental results may also be useful to investigate the nucleation and growth of multi-layer graphene. By investigating the conversion rule from small carbon rings to hexagonal or pentagonal carbon rings, as well as their nucleation and growth mechanism, the substrate-free vapor phase formation of multi-layer graphene may be easily extended to various other carbon precursors, which is promising for the large area and low cost production. Especially, the carbon precursors that directly yielding hexagonal or pentagonal carbon rings during pyrolysis are the most suitable.

#### 4. Conclusions

Large area ( $\sim\text{cm}^2$ ) synthesis of multi-layer graphene film through a substrate-free vapor phase method is presented. The SEM observation reveals that the graphene nanoflakes are six-sided and five-sided, and the internal angle between adjacent well-faced sides is nearly  $120^\circ$  and  $105^\circ$ , respectively. STM characterization exhibits the appearance of hexagonal lattice, confirming the formation of graphene layer. The nucleation of hexagonal and pentagonal carbon rings leads to carbonaceous nuclei, and grow into six-sided and five-sided nanoflakes, respectively. Then, well-ordered and large-area graphene monolayer is formed by the interconnection of six-sided and five-sided nanoflakes. Subsequently, stacking of interconnected hexagonal and pentagonal nanoflakes along the  $[0001]$  direction results in the formation of multi-layer graphene film. This approach provides an easy route for the large scale production of low cost and large area multi-layer graphene, promising for future fundamental study and technological applications.

#### REFERENCES

- [1] Lee CG, Wei XD, Kysar JW, Hone J. Measurement of the elastic properties and intrinsic strength of monolayer graphene. *Science* 2008;321(5887):385–8.
- [2] Tombros N, Jozsa C, Popinciuc M, Jonkman HT, Wees BJ. Electronic spin transport and spin precession in single graphene layers at room temperature. *Nature* 2007;448:571–4.
- [3] Berger C, Song ZM, Li XB, Wu XS, Brown N, Naud C, et al. Electronic confinement and coherence in patterned epitaxial graphene. *Science* 2006;312(5777):1191–6.
- [4] Novoselov KS, Geim AK, Morozov SV, Jiang D, Katsnelson MI, Grigorieva IV, et al. Two-dimensional gas of massless Dirac fermions in graphene. *Nature* 2005;438:197–200.
- [5] Rulter GM, Crain JN, Guisinger NP, Li T, First PN, Stroschio JA. Scattering and interference in epitaxial graphene. *Science* 2007;317(5835):219–22.
- [6] Dato A, Radmilovic V, Lee ZH, Phillips J, Frenklach M. Substrate-free gas-phase synthesis of graphene sheets. *Nano Lett* 2008;8(7):2012–6.
- [7] Sutter PW, Flege JJ, Sutter EA. Epitaxial graphene on ruthenium. *Nat Mater* 2008;7:406–11.
- [8] Somani PR, Somani SP, Umeno M. Planar nano-graphenes from camphor by CVD. *Chem Phys Lett* 2006;430(1–3):56–9.
- [9] Marchini S, Gunther S, Wintterlin J. Scanning tunneling microscopy of graphene on Ru(0001). *Phys Rev B* 2007;76(7):075429–37.
- [10] Cheng HM, Li F, Su G, Pan HY, He LL, Sun X, et al. Large-scale and low cost synthesis of single-walled carbon nanotubes by the catalytic pyrolysis of hydrocarbons. *Appl Phys Lett* 1998;72(25):3282–4.
- [11] Li WZ, Wen JG, Sennett M, Ren ZF. Clean double-walled carbon nanotubes synthesized by CVD. *Chem Phys Lett* 2003;368(3–4):299–306.
- [12] Frenklach M, Kermatick R, Huang D, Howard W, Spear KE, Phelps AW, et al. Homogeneous nucleation of diamond powder in the gas phase. *J Appl Phys* 1989;66(1):395–9.
- [13] Meyer JC, Geim AK, Katsnelson MI, Novoselov KS, Booth TJ, Roth S. The structure of suspended graphene sheets. *Nature* 2007;446:60–3.
- [14] Wang GX, Yang J, Park J, Gou XL, Wang B, Liu H, et al. Facile synthesis and characterization of graphene sheets. *J Phys Chem C* 2008;112(22):8192–5.
- [15] Stolyarova E, Rim KT, Ryu S, Maultzsch J, Kim P, Brus LE, et al. High-resolution scanning tunneling microscopy imaging of mesoscopic graphene sheets on an insulating surface. *PNAS* 2007;104(22):9209–12.
- [16] Yuan GD, Zhang WJ, Yang Y, Tang YB, Li YQ, Wang JX, et al. Graphene sheets via microwave chemical vapor deposition. *Chem Phys Lett* 2009;467(4–6):361–4.
- [17] Chen HQ, Muller MB, Gilmore KJ, Wallace GG, Li D. Mechanically strong, electrically conductive, and biocompatible graphene paper. *Adv Mater* 2008;20(18):3557–61.
- [18] Ferrai AC. Raman spectroscopy of graphene and graphite: disorder, electron–phonon coupling, doping and nonadiabatic effects. *Solid State Commun* 2007;143(1–2):47–57.
- [19] Obraztsov AN, Obraztsova EA, Tyurnina AV, Zolotukhin AA. Chemical vapor deposition of thin graphite films of nanometer thickness. *Carbon* 2007;45(10):2017–21.
- [20] Obraztsov AN, Tyurnina AV, Obraztsova EA, Zolotukhin AA, Liu BH, Chin KC, et al. Raman scattering characterization of CVD graphite films. *Carbon* 2008;46(6):963–8.
- [21] Cambaz ZG, Yushin G, Osswald S, Mochalin V, Gogotsi Y. Noncatalytic synthesis of carbon nanotubes, graphene and graphite on SiC. *Carbon* 2008;46(6):841–9.
- [22] Tang YB, Cong HT, Wang ZM, Cheng HM. Synthesis of rectangular cross-section AlN nanofibers by chemical vapor deposition. *Chem Phys Lett* 2005;416(1–3):171–5.
- [23] Lu F, Cai WP, Zhang YG. ZnO hierarchical micro/nanoarchitectures: solvothermal synthesis and structurally enhanced photocatalytic performance. *Adv Funct Mater* 2008;18(7):1047–56.
- [24] Lee ST, Peng HY, Zhou XT, Wang N, Lee CS, Bello I, et al. A nucleation site and mechanism leading to epitaxial growth of diamond films. *Science* 2000;287(7):104–6.
- [25] Balzaretta NM, Jornada JAH. High pressuring annealing of CVD diamond films. *Diamond Relat Mater* 2003;12(3–7):290–4.

- [26] Zhou B, Prorok BC, Erdemir A, Eryilmaz O. Annealing effects on the mechanical properties of near-frictionless carbon thin films. *Diamond Relat Mater* 2006;15(11–12):2051–4.
- [27] Hunter JM, Fye JL, Roskamp EJ, Jarrold MF. Annealing carbon cluster ions: a mechanism for fullerene synthesis. *J Phys Chem* 1994;98(7):1810–8.
- [28] Kiang CH, Goddard WA. Polyene ring nucleus growth model for single-layer carbon nanotubes. *Phys Rev Lett* 1996;76(14):2515–8.
- [29] Saito R, Dresselhaus G, Dresselhaus MS. Electronic structure of chiral graphene tubules. *Appl Phys Lett* 1992;60(18):2204–6.

www.spm.com.cn